Radio Science, Volume 15, Number 3, pages 559–572, May–June 1980

Model computations of radio wave scintillation caused by equatorial ionospheric bubbles

A. W. Wernik,[1] *C. H. Liu, and K. C. Yeh*

Department of Electrical Engineering, University of Illinois at Urbana-Champaign
Urbana, Illinois 61801

(Received October 25, 1979; accepted October 26, 1979.)

In situ data measured on board AE satellites and rockets reveal spiky and wedgelike electron density structures inside the equatorial ionospheric bubbles. Two models are constructed to simulate the initial stage and fully developed stage of a bubble. Effects of radio propagation through such bubbles are simulated by solving the parabolic equation numerically. The results show that even though the amplitude scintillation at 136 MHz appears to be stationary, such is not the case at gigahertz frequencies. Instead, the amplitude at gigahertz frequencies shows outbursts with large excursions whenever the direct ray intersects the spicky ionization structure. Both the peak-to-peak excursion and the amplitude distribution cannot be predicted by the scintillation theory that assumes the medium to be random.

1. INTRODUCTION

Recently, several coordinated observational campaigns at the magnetic equator have demonstrated rather convincingly the close relationship between the ionospheric bubbles and the scintillation of transionospheric radio signals [*Aarons et al.*, 1978; *Basu et al.*, 1977; *Basu and Kelley*, 1979; *Morse et al.*, 1977; *Yeh et al.*, 1979*a*, *b*]. From these joint investigations a general picture of the phenomenon has emerged. *Basu and Kelley* [1979] noted that the development of the phenomenon can be divided into several stages. Early in the evening, just after the local sunset, irregularities that cause spread *F* and VHF scintillations begin to appear below the *F* peak. Then, through some nonlinear processes these disturbances in electron density develop into regions of low density and start to rise to the topside rapidly, sometimes in a matter of several minutes, leaving behind a trail of irregularities extending to several hundred kilometers. Inside these depleted regions the so-called bubbles, irregular structures of electron density with sharp gradients exist. Sometimes wedgelike structures are found to extend upward from the *F* peak, prompting *McClure et al.* [1977] to call them 'ionization walls.' During this developed stage, radio waves propagating through these bubbles are subject to interactions with sharp gradients as well as small irregular structures of the electron density. Very intense amplitude scintillations have been observed. These bubbles appear mostly before midnight, but on many occasions they have also been observed later in local time [*Yeh et al.*, 1979*b*]. In the next stage of the development the sharp gradients as well as the turbulence start to decay, and the small-scale structures gradually disappear. In the final stage the irregularities are found to be of larger scale sizes which may still cause scintillation but will not be seen by VHF backscatter radar measurements. Theoretical explanations for the development of the various stages of the phenomenon have been presented by *Costa and Kelley* [1978], *Kelley and Ott* [1978], *Ott* [1978], and *Ossakow et al.* [1979]. Figure 1 shows an example of the apparent passage of bubbles and their effects on radio signals. The figure is a sample record of signals transmitted by Goes 1, received at Natal, Brazil (135.23°W, 5.85°S, dip −9.6°) on October 16, 1978. The signal at a frequency of 136.379 MHz is linearly polarized. The top channel is the amplitude, while the bottom two are the Faraday rotation records with one displaced by 90° from the other. An upscale in the rotation records indicates a decrease in electron content. Two isolated depletions can be seen in Figure 1, and both are accompanied by increased scintillation activity with increased fading rate and

[1] Permanent address: Space Research Centre, Polish Academy of Sciences, Warsaw, Poland.

0048-6604/80/0506-1504$01.00

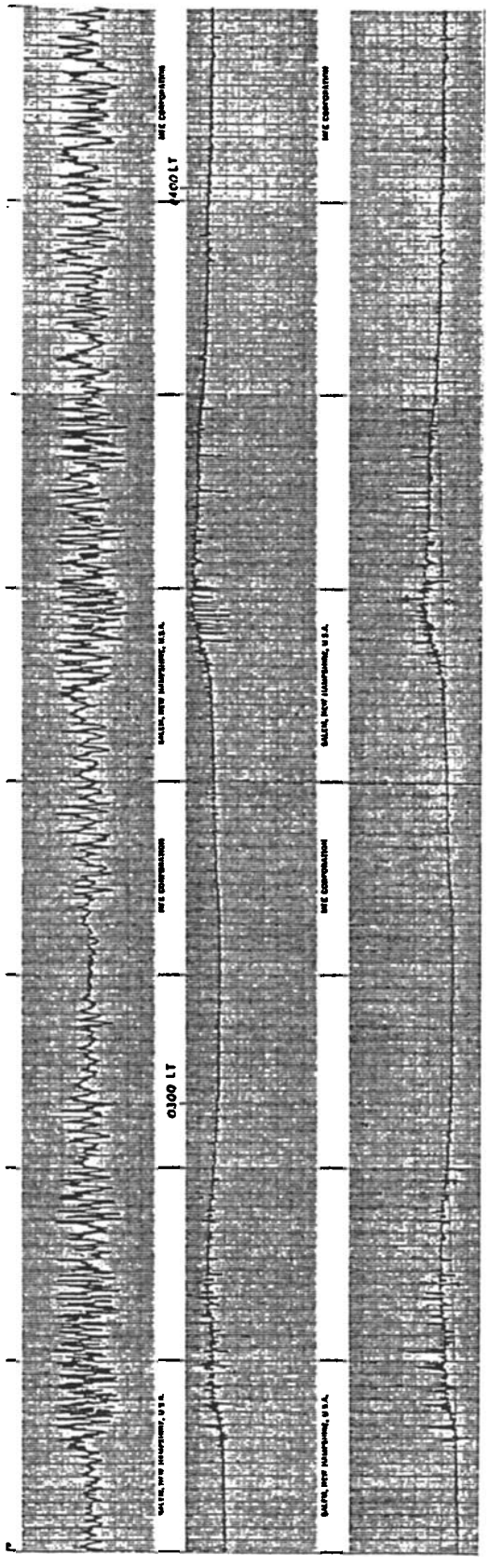

Fig. 1. Sample data of 136.379-MHz signals transmitted by the geostationary satellite Goes 1 and received at Natal, Brazil, on October 16, 1978. The top channel shows the amplitude linear in decibels with 18-db full scale. The bottom channels are the Faraday rotation in a ramp format with one channel displaced by 90° and with full scale of 180° rotation. An upscale indicates a decrease in electron content.

peak-to-peak fluctuations. From the record it is clearly seen that the signal is not stationary.

To investigate the relationship between the observed scintillation of transionospheric radio signal and these equatorial bubbles, as shown in Figure 1, one has to understand the interaction between the radio waves and the complex irregular structures of the bubbles. Most of the existing ionospheric scintillation theories are based on the statistical models of wave propagation in random media [*Ratcliffe,* 1956; *Mercier,* 1962; *Budden,* 1965; *Salpeter,* 1967; *Uscinski,* 1968; *Shishov,* 1968; *Singleton,* 1970; *Tatarskii,* 1971; *Liu et al.,* 1974; *Rumsey,* 1975; *Yeh et al.,* 1975; *Rino and Fremouw,* 1977; *Rino,* 1979]. The approach is based on the idea that the electron density structures are so complex that they can be considered random, continous distributions of irregularities. The ionosphere can then be considered a random medium whose property is characterized by a permittivity which is a random function of position and time. It is further assumed that the medium is statistically homogeneous and stationary (or, at least, locally so [*Tatarskii,* 1971]). The ergodic theorem is assumed to be valid such that experimentally observed spatial and temporal averages can be taken as ensemble averages. On the basis of these assumptions, several ionospheric scintillation theories such as thin phase screen, thick phase screen, Born and Rytov approximations, parabolic and moment equations, etc. have been developed. In all these approaches, the statistical parameter of the medium that plays the most important role is the power spectrum of the irregularities. In fact, most statistical quantities for the radio waves after they have propagated through the turbulent ionosphere are expressed in terms of the power spectrum of the irregularities. In many instances these theoretical results have been used successfully to interpret certain aspects of the observed scintillation data [*Rufenach,* 1972; *Crane,* 1976; *Umeki et al.,* 1977*a*, *b*; *Meyer et al.,* 1979; *Rino,* 1979]. However, because of the basic assumption of statistical homogeneity, there are situations for which the theoretical results may not be applicable. For example, in the fully developed stage of the equatorial bubble the electron density structures are very spiky, which hardly can be considered homogeneous. Furthermore, *Costa and Kelley* [1978] showed that although the power spectra of these structures are of power law type, they are quite different from the irregularities generated by a turbulencelike process. The sharp gradients of the observed density fluctuations are associated

with a high degree of phase coherence of their Fourier spectral components which is absent in a turbulencelike structure with the same power spectrum. If the statistical scintillation theory is applied to both cases, the same results will be obtained since the two media have the same power spectrum for the density fluctuations. Intuitively, however, the sharp gradients associated with the rapid changes in the electron density will affect the radio waves quite differently than the turbulencelike irregularities. *Crain et al.* [1979], in an effort to explain gigahertz scintillation, proposed a refractive scattering mechanism for the scintillation phenomenon in which they pointed out the importance of the sharp gradients. Thus, it seems that to understand the scintillation of radio waves through these bubbles, a different approach to the problem is required, one that does not depend on the assumption of statistical homogeneity of the medium and will take into account the effects due to the overall structures of the irregularities rather than depending solely on the power spectrum of the irregularities. One way to achieve these is to forgo the statistical characterization of the medium and avoid the equations describing the moments of the waves. Instead, one concentrates on the wave field itself and follows its evolution as it propagates through the bubble. In this paper such an approach will be followed.

Since forward scattering is still the most important factor, we shall assume that the parabolic equation for the wave field is valid. In section 2 a model describing a bubble passing through the equatorial ionosphere is constructed based on data from in situ measurements and theoretical computations. Such a model is then used in numerical solutions of the parabolic equation for radio waves propagating through the bubble. The results are discussed in section 3. In section 4 the roles the sharp gradients of the electron density profiles play in the equatorial scintillation phenomenon are investigated further. Some conclusions and discussions are made in section 5.

2. MODELING OF THE BUBBLES

To construct a model for the irregular structure of the ionospheric bubble, we took the in situ data measured by the AE-C satellite. Figure 2 shows the relative electron concentration $\Delta N/N$ along the satellite path deduced from the high-resolution ion concentration data inside a bubble [*McClure et al.*, 1977]. In modeling the concentration at the edge of the bubble was taken as the reference or as the background. To simplify later computations, we took into account the equatorial geometry and assumed a two-dimensional bubble. At each height the horizontal variations of the relative electron concentration were assumed to be given by Figure 2. For the vertical variations we made use of the results of theoretical simulations [*Ossakow et al.*, 1979]. Their numerical simulation showed that in the developing stage the leading edge of a bubble was sharpened, while the trailing edge was more blunt. To take into account such a factor, different height-dependent weighting functions shown in Figure 3 were introduced to simulate the initial and the developed stages of a bubble. These functions were multiplied by the horizontal variations of $\Delta N/N$ to yield the two-dimensional model for the bubble. In addition, the background density corresponding to the concentration at the edge of the bubble was allowed to change with height also. In particular, a parabolic profile

$$N(z) = N_0 [1 - (z - z_0)^2/H^2] \tag{1}$$

was adopted, where N_0 was the maximum electron concentration at the height z_0 and H was the scale height. Figures 4 and 5 show examples of electron concentration variations ΔN at several altitudes inside the bubble in the initial stage and the developed stage, respectively.

The model does not take into account any possible small-scale vertical variations of the electron concentration. However, it does possess the main features of vertically extended sharp gradients in electron density. In the next section these models will be used in our computations to find the structures of the wave fields after they have propagated through the bubble.

3. RADIO WAVE PROPAGATION THROUGH THE BUBBLE

Let us now consider the following situation. A plane electromagnetic wave propagating in the z direction is incident on a bubble from above. The field can be written as

$$E = u(\rho, z) \exp(-jkz) \tag{2}$$

where u is the complex amplitude for the wave

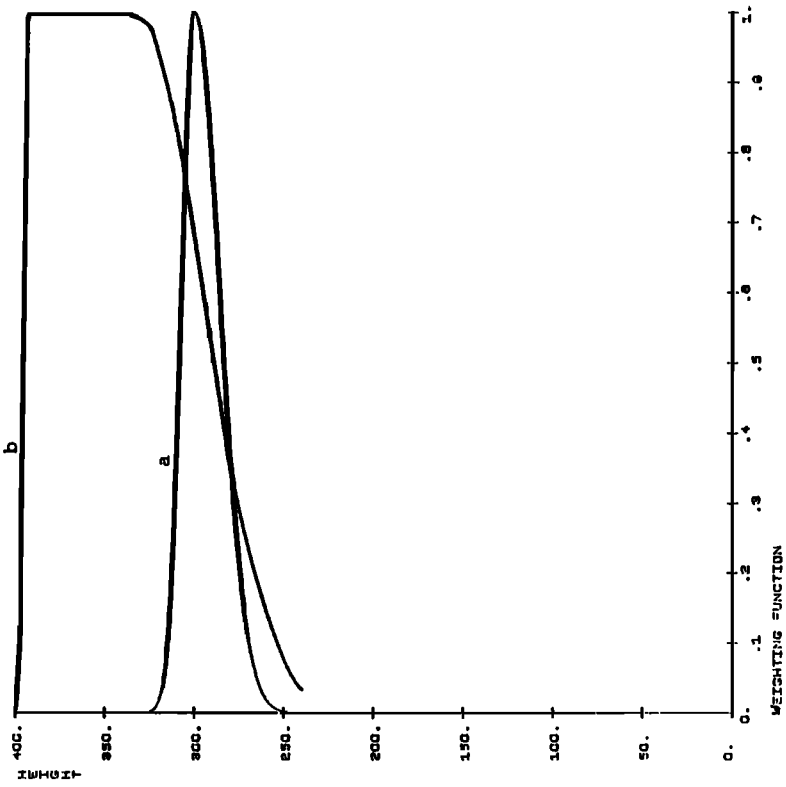

Fig. 3. Weighting functions used to model (*a*) 'initial stage' and (*b*) 'developed stage' of the plasma bubble.

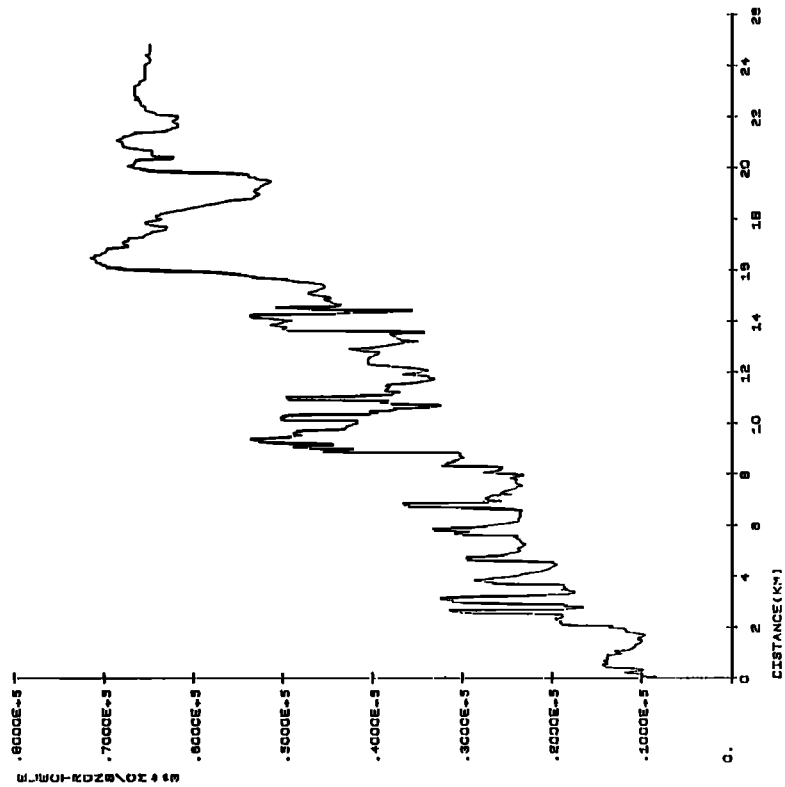

Fig. 2. High-resolution electron density profile measured inside the plasma bubble by AE-C. (The figure is reconstructed from one given by *McClure et al.* [1977] after digitization.)

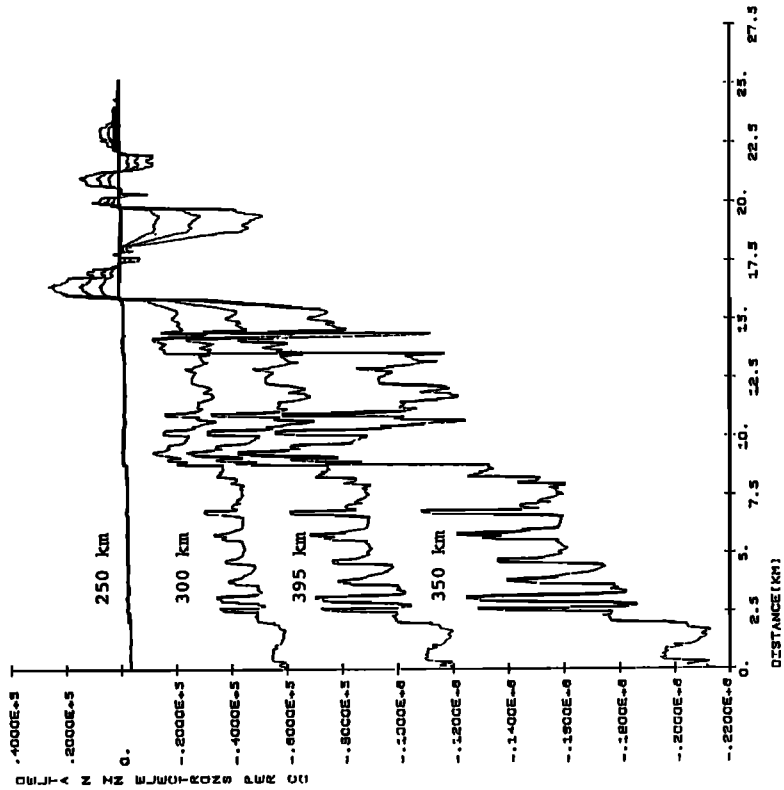

Fig. 5. Same as Figure 4 for a bubble in the developed stage.

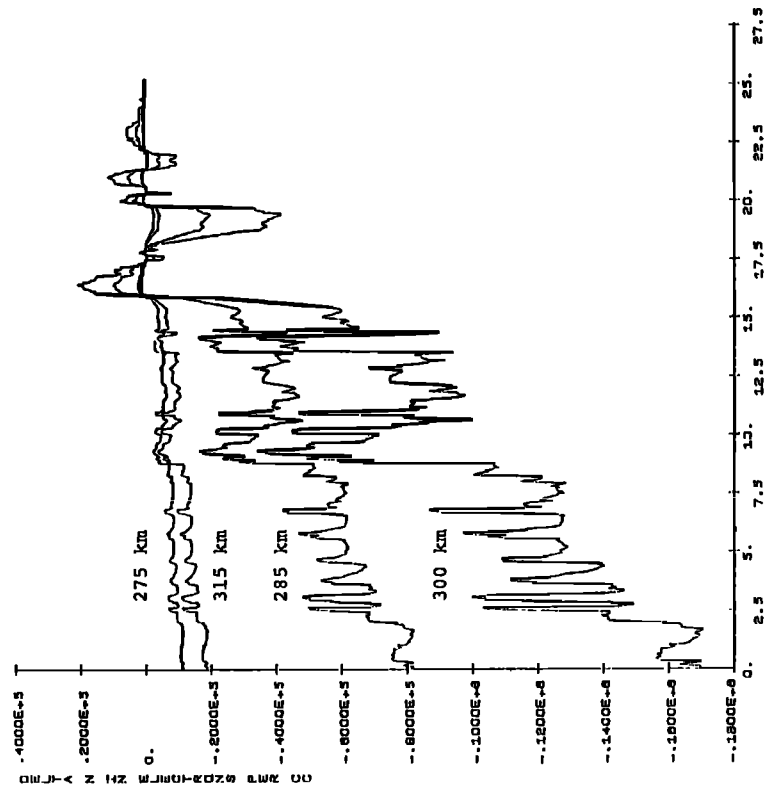

Fig. 4. Horizontal electron density fluctuation profiles at different heights inside a model bubble in its initial stage.

and is a constant for the incident wave and k is the wave number corresponding to the background ionosphere. The complex amplitude satisfies the parabolic equation [*Tatarskii,* 1971]

$$-2jk\frac{\partial u}{\partial z} + \nabla_T^2 u + k^2 \varepsilon_1 u = 0 \tag{3}$$

where ε_1 is the fluctuating part of the dielectric permittivity that is caused by the presence of the bubble. It is given by

$$\varepsilon_1(r) = -\frac{e^2 \Delta N(\mathbf{r})}{m\varepsilon_0 \omega^2} \tag{4}$$

where e and m are the electron charge and mass, respectively, ε_0 is the free space permittivity, and $\Delta N(\mathbf{r})$ is the fluctuation in electron concentration. The term ∇_T^2 in (3) is the transverse Laplacian, and for the two-dimensional model we are working with it reduces to $\partial^2/\partial x^2$.

To investigate the field distribution as the wave propagating through the bubble, (3) will be solved using the models of ΔN described in the previous section. With such complicated variations in ΔN the parabolic equation can only be solved numerically. A numerical code adopting an implicit method generalized from the Crank-Nicholson scheme [*Ames,* 1977] has been developed. The scheme is stable and quite efficient in that rather large steps in the z direction (up to 1 km) can be used. The code was checked by applying it to the solution of diffraction by an isolated Gaussian irregularity. The results agree well with those obtained from the diffraction integrals. The data for ΔN are digitized every 42 m, which is slightly greater than the sampling interval of the in situ measurements. This sets the lower limits on the irregularity scale size and the sharpness of the gradient. It is still much less than the Fresnel zone dimension for a typical distance between the bottom of the bubble and the receiver on the ground (200 to ~300 km) for wave frequencies up to several gigahertz. Different models for the bubble are substituted in (4) to obtain the numerical values for ε_1, and then (3) is solved with the initial condition that $u = 1$ for the incident wave. Figure 6 shows the results for a wave of 1.5 GHz passing through a bubble in its initial stage. The horizontal variations of the electron density ΔN at four different levels inside the bubble are those given in Figure 4. The bubble is assumed to be 50 km wide and symmetrical. The bubble thickness, defined as distance between levels at which the weighting function falls to e^{-1}, is $L = 30$ km for this initial stage. The parameters for the background ionosphere are $z_0 = 350$ km, $H = 110$ km, and $N_0 = 2.5 \times 10^5$ electrons/cm^3. We note from Figure 4 that the largest horizontal variation across the bubble occurs at an altitude of about 300 km. In Figure 6 the real and imaginary components of the complex amplitude of the wave as well as the amplitude and the phase at ground level about 250 km from the bottom of the bubble are shown as functions of horizontal distance. The nonstationary nature of the amplitude and phase record is quite obvious. But the most interesting feature in this result is the close correspondence between the positions of strong amplitude outbursts and the locations of sharp electron density gradients shown in Figure 2. This seems to support the idea that the sharp gradients have strong effects on the wave fields. This point will be examined in more detail in a later section.

For a developed bubble the layer thickness increases to $L = 115$ km, and the maximum ΔN is also increased as shown in Figure 5. Figure 7 shows the ground level complex amplitude of the 1.5-GHz wave after it has passed through such a developed bubble. The fluctuations are seen to have increased as compared to those in Figure 6, although the background ionosphere remains the same. The thicker dimension of the developed bubble as well as the greater fluctuations of ΔN contribute to the increased scintillation. Strong amplitude fluctuations associated with the sharp gradients are still observed, although they are somewhat obscured by the contributions of scattering from small irregularities. Figure 8 shows the amplitude fluctuations of the wave at ground level for the initial bubble at several frequencies. The effects of the sharp gradients are apparent for 800-MHz, 1.5-GHz, and 4-GHz signals. Figure 9 shows the same amplitudes for the developed bubble. Comparing Figures 8 and 9, it is interesting to note the increase in the fading rate as the bubble thickens from the initial stage to the developed stage. This agrees well with the measurements showing increasing amplitude fading rate as the bubble develops and extends above the F peak [*Basu et al.,* 1977]. The inhomogeneous features of the structures inside the bubble are also reflected in these amplitude plots. At the edges of the bubble (distance greater than 15 km), scintillation intensity and fading rate are smaller

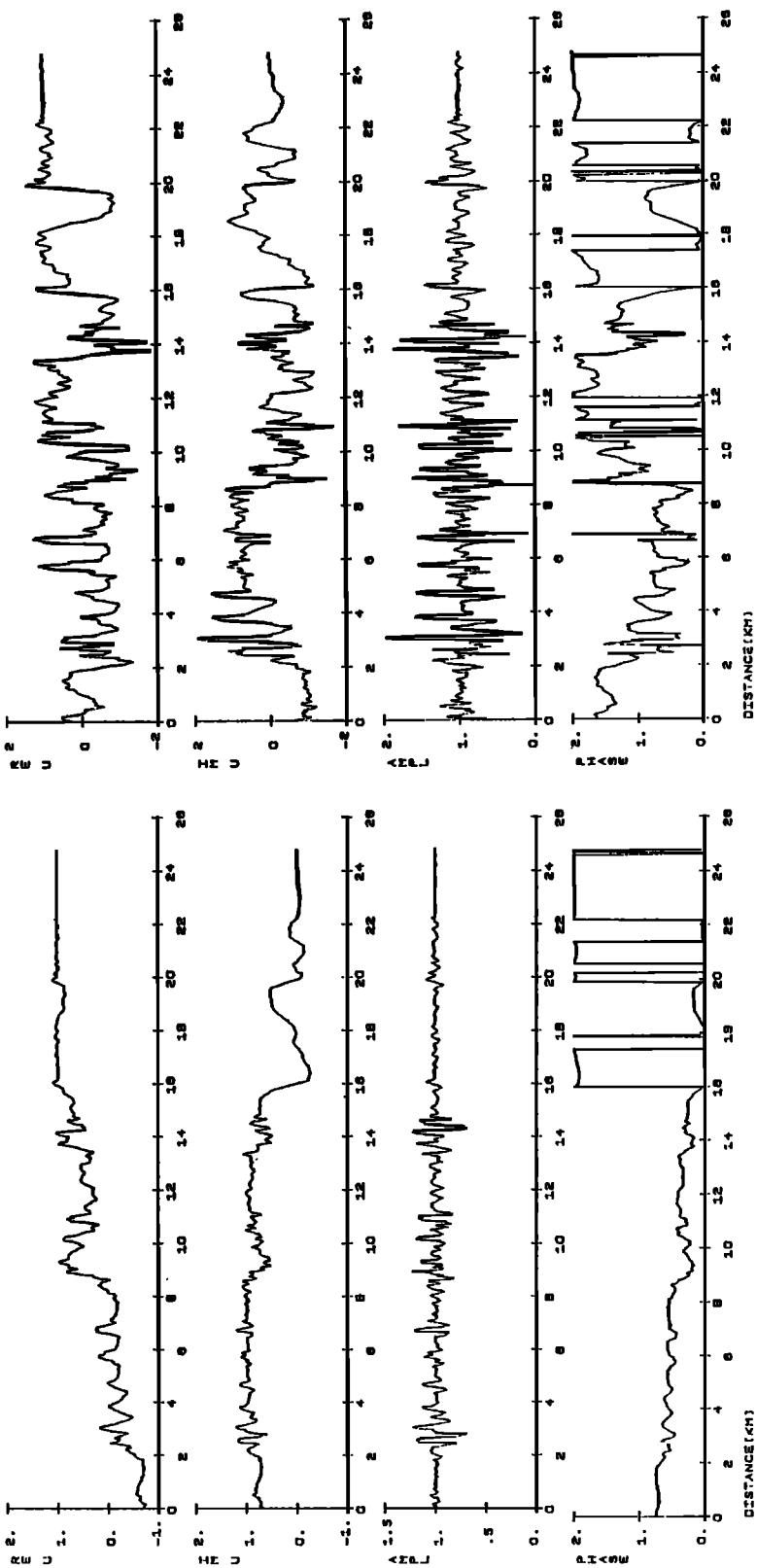

Fig. 6. Plots of the real and imaginary components of the complex amplitude, amplitude, and phase (in π units) of a wave passing through the initial stage bubble and received on the ground. The wave frequency is 1500 MHz. Horizontal distance is measured from the projection of the center of the bubble on the ground.

Fig. 7. Same as in Figure 6 but for the bubble in the developed stage.

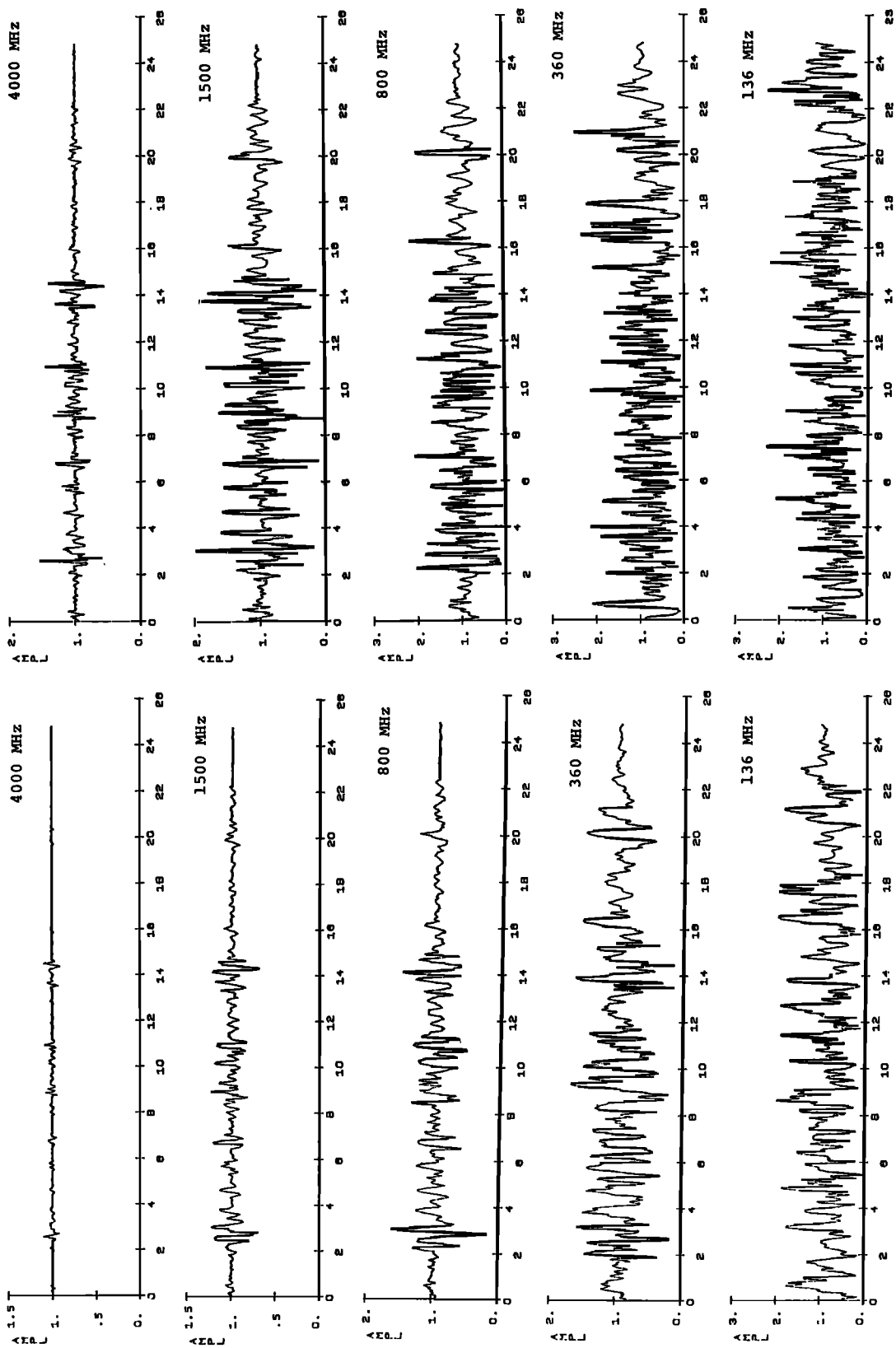

Fig. 8. Amplitude pattern at different frequencies produced by the initial stage bubble.

Fig. 9. The same as in Figure 8 but for the developed stage bubble.

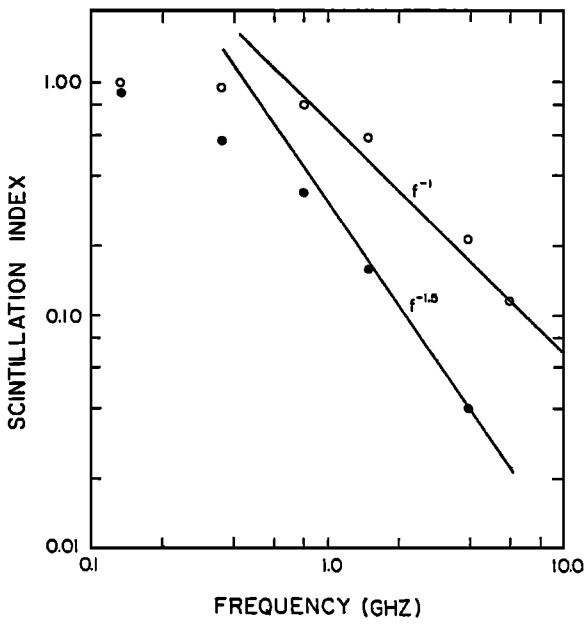

Fig. 10. Scintillation index frequency dependence for the initial (solid circles) and developed (open circles) bubble stages.

than they are closer to the center. Although the computed amplitude pattern is nonstationary especially at higher frequencies, it may be of interest to compute the scintillation index S_4 for the segments of the data which are roughly stationary. Between $x = 0$ and 15 km, S_4 indices computed for every 5-km data segment differed not more than 25%. The average was used to study the frequency dependence of S_4. Figure 10 shows the results from the computation. For weak scintillations, S_4 is proportional to $f^{-\nu}$ with the spectral index ν close to 1.5. For moderately strong scintillations ($S_4 < 0.5$), ν is between 1 and 1.5. Saturation becomes the dominant factor for strong scintillation cases. This frequency dependence is consistent with the observational data [*Taur*, 1976]. Thus by using the models for the bubble developed from in situ data and simulation results, we have shown that scintillation patterns similar to those observed experimentally are obtained when radio waves propagate through those bubbles. Many of the features in the observational data can be found in the computed results.

4. EFFECTS OF SHARP GRADIENTS IN ELECTRON DENSITY

As shown in the computational results, the sharp gradients in electron density have rather pronounced effects on the received signal, especially at higher frequencies. This can be seen more clearly in Figure 11, where the gradient of the electron density variations is plotted together with the amplitudes of 4- and 1.5-GHz radio waves that have passed through the developed bubble and received on the ground. The sudden outbursts of amplitude fluctuations coincide very well with the positions where sharp gradients exist. In this section this point will be investigated further to show the possible connections between the sharp gradients and the gigahertz scintillation phenomenon.

As pointed out in the introduction, the results derived from the statistical theory of scintillation depend mainly on the power spectrum of the irregularities. However, it has been demonstrated by *Costa and Kelley* [1978] that inhomogeneous structures with sharp gradients also have power law type of spectra, as the turbulencelike irregularities do. Therefore if statistical scintillation theory is applied to find the statistical characteristics of waves passing through inhomogeneous structures with sharp gradients, the results will be the same as if the waves had passed through a region of turbulencelike irregularities. On the other hand, in our model computations it is possible to study the distributions of the wave fields as they propagate through the two types of inhomogeneities and check if they have the same statistical characteristics. To do this, we follow the procedure used by *Costa and Kelley* [1978] to obtain a model for a bubble filled with turbulencelike irregularities that has the same power spectrum as the original electron density variations from the in situ measurements. When the original in situ data for the electron density were Fourier analyzed, the amplitude of the Fourier coefficients follow a κ^{-1} power law behavior as shown in Figure 12, indicating a κ^{-2} dependence for the power spectrum. This is a typical in situ measured electron density spectrum in the F region [*Dyson et al.*, 1974]. If the amplitudes of the Fourier components are kept the same, while a random phase angle ($0 - 2\pi$) is added to the phase of each Fourier component and then transformed back to the spatial domain, we will obtain a turbulencelike distribution of irregularities. The power spectrum of this distribution is the same as the original one, but it has very little phase coherence in its spectral components. Several such bubbles have been generated. An example is shown in Figure 13. We note the absence of the sharp spikes which were present in the original data in Figure 2. Instead, more weak,

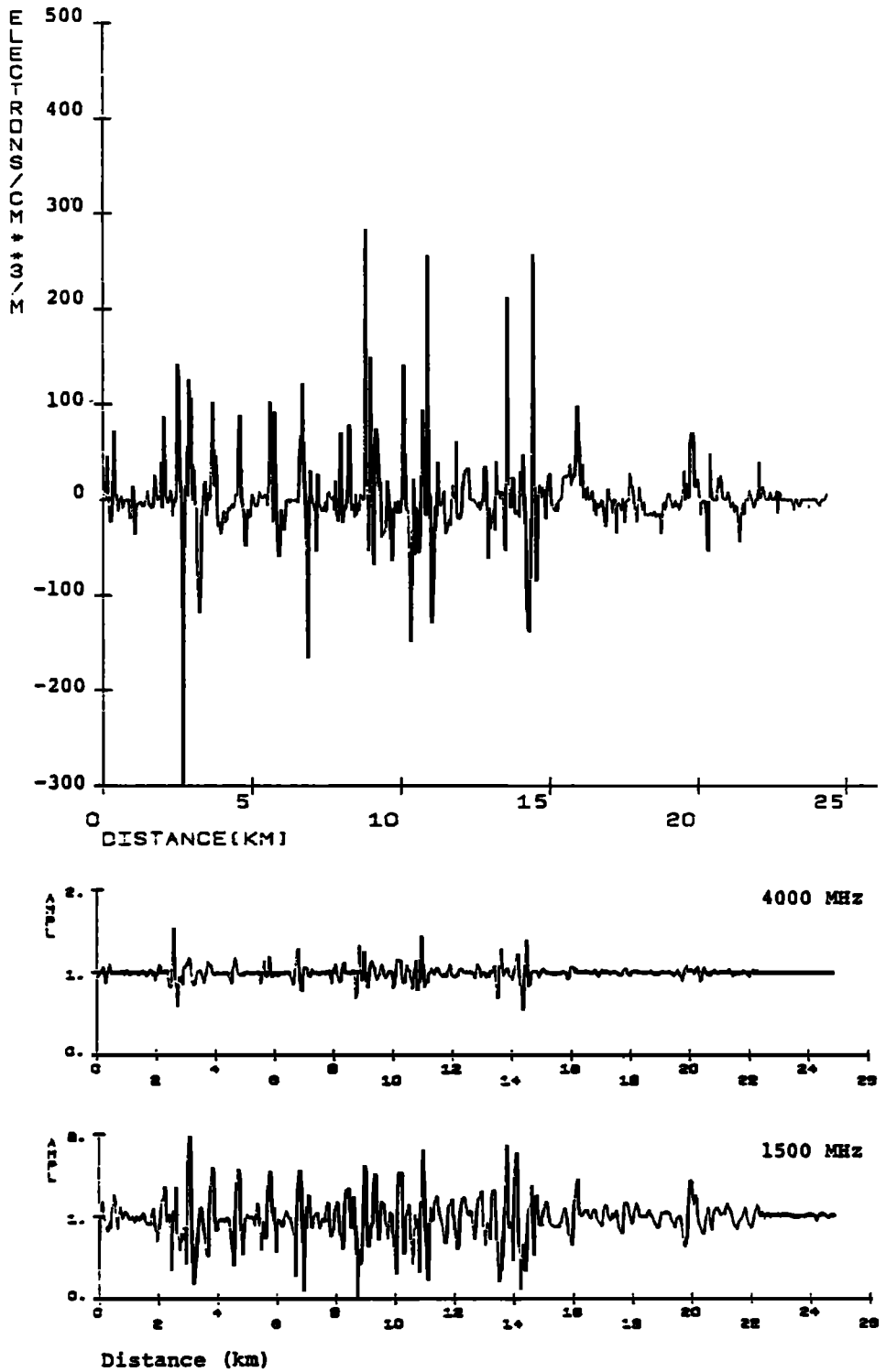

Fig. 11. Comparison of the variations of the gradients of the electron density inside the bubble with the ground level amplitudes of 4- and 1.5-GHz waves passed through the developed bubble. Sharp gradients coincide with sudden outbursts of amplitude fluctuations.

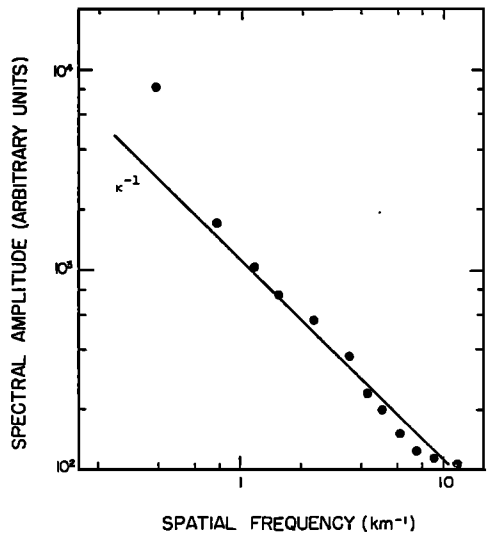

Fig. 12. Amplitude of the Fourier components of the electron density fluctuations inside the bubble.

small-scale structures are seen in Figure 13. These models were then used in the numerical code to solve for the wave field distributions for different frequencies. Figure 14 shows some sample results for such computations at 4 GHz and 360 MHz. Comparing to those obtained for the original density structures as shown in Figure 8, we note that the amplitude fluctuations are more stationary. The scintillation indices S_4 computed for the signals in Figure 14 are 0.021 for 4 GHz and 0.48 for 360 MHz. The corresponding S_4 for the original profile are 0.04 and 0.64, respectively. This difference in scintillation intensity can be attributed only to the sharp gradients present in the original profile, since the power spectra for the two cases are the same. The increase is more apparent at the high frequencies. This seems to be due to the fact that at 4 GHz the main contribution to the amplitude fluctuation comes from the sharp gradients, while at lower frequencies other small irregularities may also contribute to the overall amplitude scintillation. Therefore when the sharp gradients are eliminated by randomizing the phase, the scintillations at gigahertz frequencies are more drastically reduced. This then leads to the conclusion that bubbles with sharp electron density gradients are rather efficient in producing observable scintillations at gigahertz frequencies.

Figure 15 shows the histograms for the amplitude distributions for the two cases. For the original profile the amplitude fluctuations span a much wider band than those for the randomized medium. At the same time, there is a larger peak about the mean value of one for the original bubble. This is consistent with the fact that for the original bubble there is not much random scattering due to small-scale irregularities; rather the sharp gradients are mainly responsible for the larger-amplitude excursions.

Similar computations have been made for several other bubbles generated by the phase randomization procedure. The results are all consistent with the general picture discussed above.

5. CONCLUSIONS

In this paper the problem of radio wave scintillation caused by equatorial ionospheric bubbles is studied using model computations. The models for the bubbles are constructed from in situ measured electron density data and from results obtained in numerical simulations. It is noted that the density variations inside a bubble can at times be very spiky. Sharp gradients make the medium highly inhomogeneous in the statistical sense. Therefore the existing statistical scintillation theory may not be applicable to studying the problem. Instead, these models are used in a direct solution of the parabolic equation to obtain the distribution of the wave fields. The inhomogeneous nature of the medium causes the wave fields to be nonstationary. Many of the features in the observed data are reproduced in our computed results. The most interesting point coming out of the computational results is the fact that sharp gradients in electron density variations affect the field distributions in a way quite different from the way in which the small irregularities do. Sharp large outbursts of amplitude fluctuations are seen to occur at the places where sharp gradients of the density exist. These effects are more pronounced at higher frequencies, namely, the gigahertz frequencies in our computations. The point is further supported by our results when waves are propagated through bubbles generated by randomly mixing the phases of the Fourier components of the original density variations. The results indicate that when the sharp gradients are eliminated in the density variations by the phase randomization, no sudden outbursts of amplitude fluctuations appear, and the scintillation indices are reduced, although the power spectra of the irregularities are

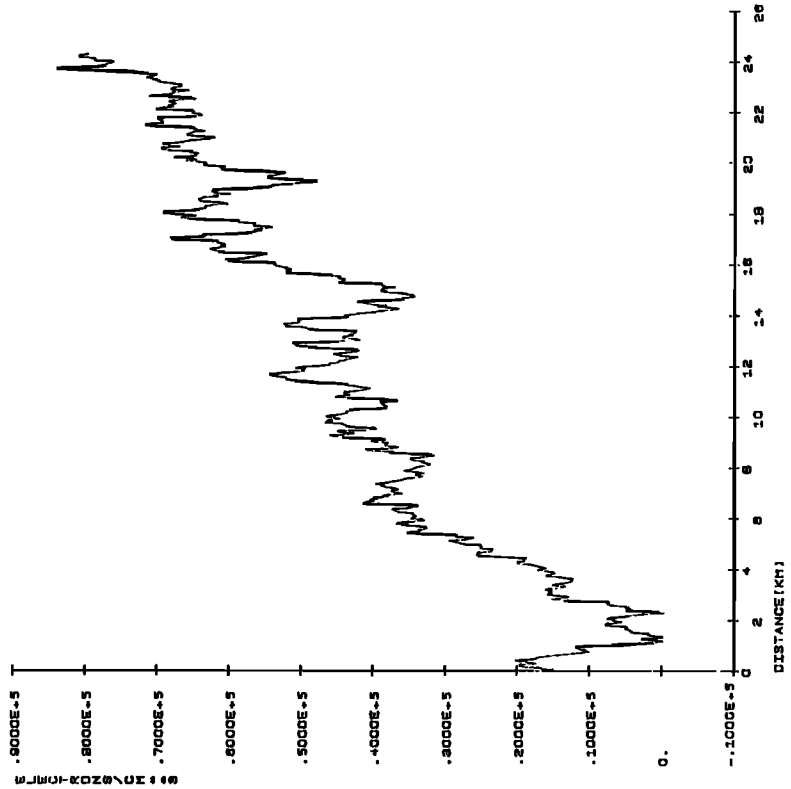

Fig. 13. Horizontal electron density variations obtained by randomizing phases of the Fourier components of the data shown in Figure 2.

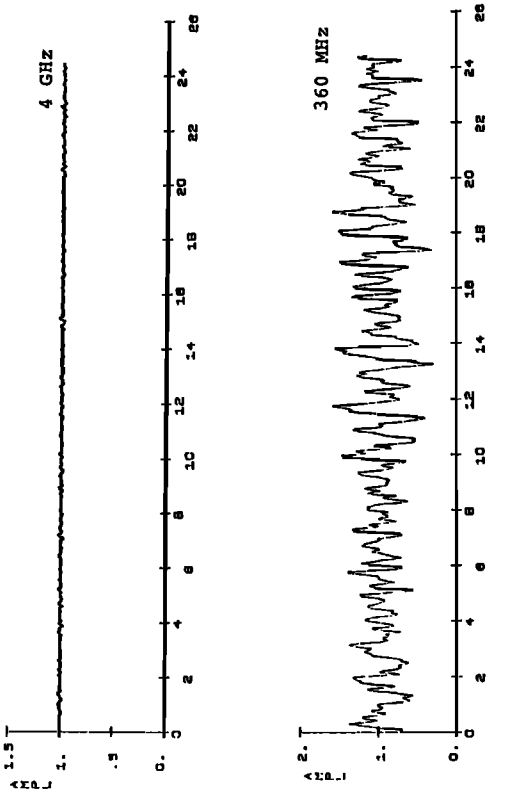

Fig. 14. Amplitude scintillation pattern at 360 MHz and 4000 MHz produced by the initial stage bubble with the horizontal structure shown in Figure 13.

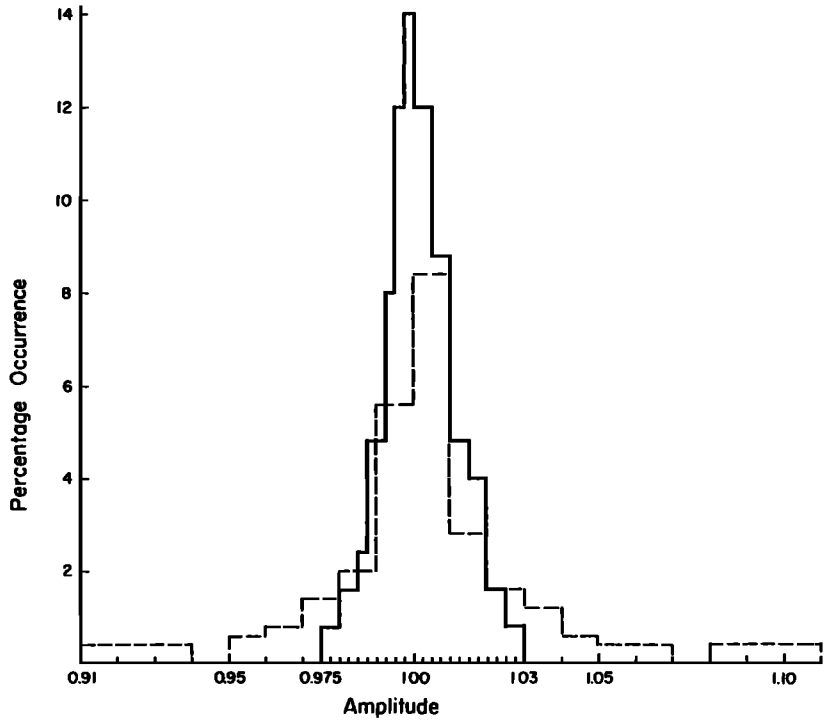

Fig. 15. Histograms showing the distributions of the amplitudes of the 4-GHz signals for the original density distribution (dashed lines) and the randomized density distribution (solid lines). The histograms are normalized such that the areas under the two curves are the same.

still the same. It is therefore clear that the sharp gradients are the major causes of scintillations of gigahertz radio waves propagating through bubbles. For these cases where wedgelike electron walls exist, the scintillation theory based on the power spectrum of the irregularities is inadequate. Our direct approach offers a procedure that does not depend on the assumption of statistical homogeneity of the medium. It also takes into account such inhomogeneous features of the medium as the extended wedgelike structures.

The results of these computations are consistent with our physical intuitions. In general, fluctuations of wave field depend on the fine structure within about one Fresnel radius of the direct path. At a frequency of approximately 100 MHz this radius is more than 1 km, within which substantial structure can be seen (refer to Figure 2). Consequently, the computed amplitude should show more or less stationarity as expected. As the frequency is raised to above 1 GHz, the Fresnel radius shrinks to 300 m or less. Inside this smaller Fresnel zone the radio rays will fall through either smooth and slow change in electron density, in which case little scintillation will be created, or spiky electron density wedges, in which case edge diffraction effects are strong and large excursions in amplitude are expected. As a result the gigahertz frequency amplitudes are expected to be nonstationary and to show sudden outbursts with an amplitude distribution shown in Figure 15. When the irregularity structure is Fourier analyzed and its phase randomized, the reconstructed bubble will have small irregularities distributed uniformly. The diffraction of waves from such a reconstructed bubble will produce a stationary field even at gigahertz frequencies, and their scintillation levels are generally reduced from the case when bubbles are composed of spiky structures.

The model we constructed for the bubble is very simple and is far from perfect. In particular, it is two-dimensional and does not take into account any small-scale vertical variations in the electron density profile. However, it does contain the important features we wish to study. A more realistic model will depend on the availability of simultaneous experimental data in a three-dimensional

bubble. The scale of such a measurement program will be enormous, and the model of thusly produced three-dimensional bubbles is consequently not expected in the foreseeable future. However, the crude model used in this paper can certainly be improved as more experimental data are made available.

Acknowledgments. This work was supported in part by a grant ATM 77-22485 from the Atmospheric Research Sections, National Science Foundation, and in part by the Air Force Geophysics Laboratory under contract F19628-78-C-0195.

REFERENCES

Aarons, J., J. Buchau, S. Basu, and J. P. McClure (1978), The localized origin of equatorial *F* region irregularity patches, *J. Geophys. Res., 83,* 1659–1664.

Ames, W. F., *Numerical Methods for Partial Differential Equations,* Academic, New York, 1977.

Basu, S., and M. C. Kelley (1979), A review of recent observations of equatorial scintillations and their relationship to current theories of *F*-region irregularity generation, *Radio Sci., 14,* 471–485.

Basu, S., J. Aarons, J. P. McClure, C. Lahoz, A. Bushby, and R. F. Woodman (1977), Preliminary comparisons of VHF radar maps of *F*-region irregularities with scintillations in the equatorial region, *J. Atmos. Terr. Phys., 39,* 1251–1262.

Budden, K. G. (1965), The amplitude fluctuations of the radio wave scattered from a thick ionospheric layer with weak irregularities, *J. Atmos. Terr. Phys., 27,* 155–172.

Costa, E., and M. C. Kelley (1978), On the role of steepened structures and drift waves in equatorial spread *F*, *J. Geophys. Res., 83*(A9), 5359–4364.

Crain, C. M., H. G. Booker, and J. A. Ferguson (1979), Use of refractive scattering to explain SHF scintillation, *Radio Sci., 14,* 125–134.

Crane, R. K. (1976), Spectra of ionospheric scintillation, *J. Geophys. Res., 81,* 2041–2050.

Dyson, P. L., J. P. McClure, and W. B. Hanson (1974), In situ measurements of the spectral characteristics of *F* region ionospheric irregularities, *J. Geophys. Res., 79,* 1497–1502.

Kelley, M. C., and E. Ott (1978), Two-dimensional turbulence in equatorial spread *F*, *J. Geophys. Res., 83,* 4369–4372.

Liu, C. H., A. W. Wernik, K. C. Yeh, and M. Y. Youakim (1974), Effects of multiple scattering on scintillation of trans-ionospheric radio signals, *Radio Sci., 9,* 599–607.

McClure, J. P., W. B. Hanson, and J. H. Hoffman (1977), Plasma bubbles and irregularities in the equatorial ionosphere, *J. Geophys. Res., 82,* 2650–2656.

Mercier, R. P. (1962), Diffraction by a screen causing large random phase fluctuations, *Proc. Cambridge Phil. Soc., 58,* 382–400.

Meyer, W. J., R. J. Gjeldum, C. H. Liu, and K. C. Yeh (1979), A study of ionospheric scintillations of phase and quadrature components, *J. Geophys. Res., 84,* 2039–2048.

Morse, F. A., B. C. Edgar, H. C. Koons, C. J. Rice, W. J. Heikkila, J. H. Hoffman, B. A. Tinsley, J. D. Winningham, A. B. Christensen, R. F. Woodman, J. Pomalaza, and N. R. Teixeira (1977), Equion: An equatorial ionospheric irregularity experiment, *J. Geophys. Res., 82,* 578–592.

Ossakow, S. L., S. T. Zalesak, B. E. McDonald, and P. K. Chaturvedi (1979), Nonlinear equatorial spread *F*: Dependence on the altitude of the *F* peak and bottomside background electron density gradient scale length, *J. Geophys. Res., 84,* 17–23.

Ott, E. (1978), Theory of Rayleigh-Taylor bubbles in the equatorial ionosphere, *J. Geophys. Res., 83,* 2066–2070.

Ratcliffe, J. A. (1956), Some aspects of diffraction theory and their application to the ionosphere, *Rep. Progr. Phys., 19,* 188–267.

Rino, C. L. (1979), A power-law phase screen model for ionospheric scintillation, 1, 2, *Radio Sci., 14,* 1135–1155.

Rino, C. L., and E. J. Fremouw (1977), The angle dependence of singly scattered wavefields, *J. Atmos. Terr. Phys., 39,* 859–868.

Rufenach, C. L. (1972), Power law wave number spectrum deduced from ionospheric scintillation observations, *J. Geophys. Res., 77,* 4761–4772.

Rumsey, V. H. (1975), Scintillations due to a concentrated layer with a power-law turbulence spectrum, *Radio Sci., 10,* 107–114.

Salpeter, E. E. (1967), Interplanetary scintillations, 1, Theory, *Astrophys. J., 147,* 433–448.

Shishov, V. J. (1968), Theory of wave propagation in random media, *Radiophys. Quantum Electron., 11,* 500–505.

Singleton, D. G. (1970), Saturation and focusing effects in radiostar and satellite scintillations, *J. Atmos. Terr. Phys., 32,* 187–196.

Tatarskii, V. I. (1971), The effects of the turbulent atmosphere on wave propagation, report. (Available from National Technical Information Service, Springfield, Va.)

Taur, R. R. (1976), Simultaneous 1.5- and 4-GHz ionospheric scintillation measurements, *Radio Sci., 11,* 1029.

Umeki, R., C. H. Liu, and K. C. Yeh (1977*a*), Multifrequency spectra of ionospheric amplitude scintillations, *J. Geophys. Res., 82,* 2752–2760.

Umeki, R., C. H. Liu, and K. C. Yeh (1977*b*), Multifrequency studies of ionospheric scintillations, *Radio Sci., 12,* 311–317.

Uscinski, B. J. (1968), The multiple scattering of waves on irregular media, *Phil. Trans. Roy. Soc. London, Ser. A, 262,* 609–640.

Yeh, K. C., C. H. Liu, and M. Y. Youakim (1975), A theoretical study of the ionospheric scintillation behavior caused by multiple scattering, *Radio Sci., 10,* 97–106.

Yeh, K. C., H. Soicher, C. H. Liu, and E. Bonelli (1979*a*), Ionospheric bubbles observed by the Faraday rotation method at Natal, Brazil, *Geophys. Res. Lett., 6,* 473–475.

Yeh, K. C., H. Soicher, and C. H. Liu (1979*b*), Observations of equatorial ionospheric bubbles by the radio propagation method, *J. Geophys. Res., 84,* 6589–6594.